PRODUCING SEAMLESS GLOBAL MOSAICS OF TITAN WITH THE VIMS IMAGING SPECTROMETER

S. Le Mouélic[1], T. Cornet[2], S. Rodriguez[3], C. Sotin[1,4], J. W. Barnes[5], R. H. Brown[6], K. H. Baines[4], B. J. Buratti[4], R. N. Clark[7], P. D. Nicholson[8]. [1]Laboratoire de Planétologie et de Géodynamique, UMR 6112, CNRS, Université de Nantes, 2 rue de la Houssinière, 44322 Nantes, France. [2]ESA/ESAC, Villanueva de la Canada, Spain. [3]Laboratoire AIM, Centre d'étude de Saclay, IRFU/Sap, Centre de l'Orme des Merisiers, Gif/Yvette, France. [4]Jet Propulsion Laboratory, California Institute of Technology, 4800 Oak Grove Drive, Pasadena, CA 91109, USA. [5]Department of Physics, University of Idaho, Engineering-Physics Building, Moscow, ID 83844, USA. [6]Department of Planetary Sciences, University of Arizona, Tucson, AZ 85721, USA. [7]Planetary Science Institute, Tucson, USA. [8]Department of Astronomy, Cornell University, Ithaca, NY 14853, USA. (stephane.lemouelic(at)univ-nantes.fr).

Introduction: The Visual and Infrared Mapping Spectrometer (VIMS) onboard Cassini observes the surface of Titan in seven narrow atmospheric windows in the infrared at 0.93, 1.08, 1.27, 1.59, 2.01, 2.68-2.78, and 4.9-5.1 microns [1,2]. We have produced a global hyperspectral mosaic at 32 pixels per degres of the complete VIMS data set of Titan between T0 (July 2004) and T113 flyby (Sep. 2015). We merged all the data cubes sorted by increasing spatial resolution, with the high resolution images on top of the mosaic and the low resolution images used as background.

Methodology and results: Many seams appear between individual images in the raw global mosaic of Titan at 2 µm (Fig 1a). They are mainly caused by the varying vewing angles (incidence i, emission e, phase/azimut g/ϕ) between data acquired during the different Titan flybys. These angles induce significant surface photometric effects and a strongly varying atmospheric (absorption and scattering) contribution, the scattering of the atmosphere being all the more present than the wavelength is short.

We first filtered out the observing geometry in order to remove the pixels acquired in too extreme illuminating and viewing conditions. We used thresholds of 80° both on the incidence and emission angles, 120° on the phase angle, and 7 on the airmass (defined by 1/ cos i + 1/cos e). These thresholds corresponds to a trade-off between surface coverage (in particular in polar areas) and data quality. The viewing geometry is normalized at first order using a lambertian surface photometric function derived from the observation at 5 µm, where the atmospheric scattering is almost negligible [3,4]. Dividing the data by cos i normalizes the illuminating conditions for the 5 µm window, but this correction alone is not efficient for windows shorter than the 5 µm one (Fig. 1b). This is mainly due to an additive scattering contribution of the atmosphere.

To mitigate this effect, we use the wings of the atmospheric windows as a proxy to correct for the amount of additive scattering present in the center of these windows, where the surface is seen by VIMS [4]. The resulting global map at 2 µm empirically corrected from scattering and photometry is shown in Fig 1c. The level of residual seams has been significantly decreased.

To investigate spectral heterogeneities, RGB composites of band ratios generally prove to be more efficient to highlight subtle variations than RGB composites of single bands only. This is particularly true when no spurious additive term is present (either instrumental such as the dark, or physical such as the scattering), as ratios cancel out the effects of multiplicative terms, such as the photometric function. For Titan, using band ratios is still challenging, as they are also generally much more sensitive to residual calibration artifacts and atmospheric residuals. Fig. 2a presents a global color map with the red, green and blue controlled by the 5, 2 and 1.27 µm images corrected at first order from scattering and photometry. Orthographic views of this map are given Fig. 3, with zooms on Sinlap crater and the Huygens landing site, where features imaged by DISR at the beginning of its descent can be easily recognized (bottom part of the image). Fig. 2b presents the 2.03/1.27 µm ratio. Fig. 2c corresponds to a RGB composite of the 1.59/1.27 µm, 2.03/1.27 µm and 1.27/1.08 µm ratios. Whereas the strongly diffusing atmosphere hampers the study of the polar areas (appearing in pink), the ratios nicely reveal the extent of equatorial dune fields appearing in brownish tones.

Conclusion and perspectives : The residual discrepancies in the map can be attributed to several factors, which we plan to correct in further studies. Possible cloud contributions could be removed using the cloud spectral detection algorithm proposed by [5]. Several cubes around Kraken Mare contain specular reflections that could also be filtered out [6]. Temporal variations at the surface, as observed by [7], might also be present in the 11 years of data integrated in this map. The surface photometric behavior can be significantly improved using a more complex photometric function, including the emergence and phase angles [8]. Finally, more inputs derived from a complete radiative transfer analysis [9] could also provide another way to improve the homogeneity of the maps.

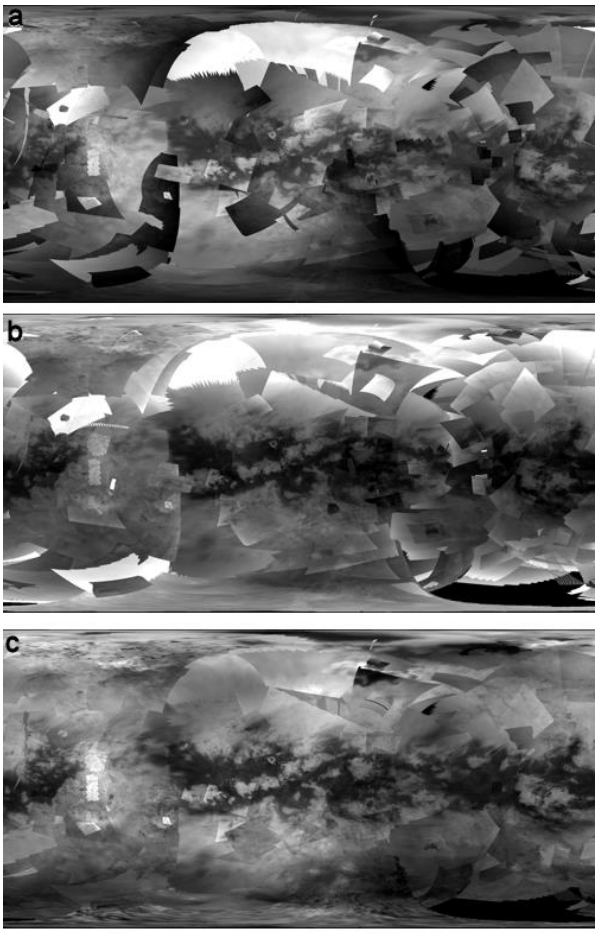

Fig.1 : Global maps of Titan using data from Ta (10/2004) to T113 (09/2015). (a) I/F at 2µm. (b) I/F divided by cos i. (c) I/F corrected from scattering before dividing by cos i, to reduce the seams..

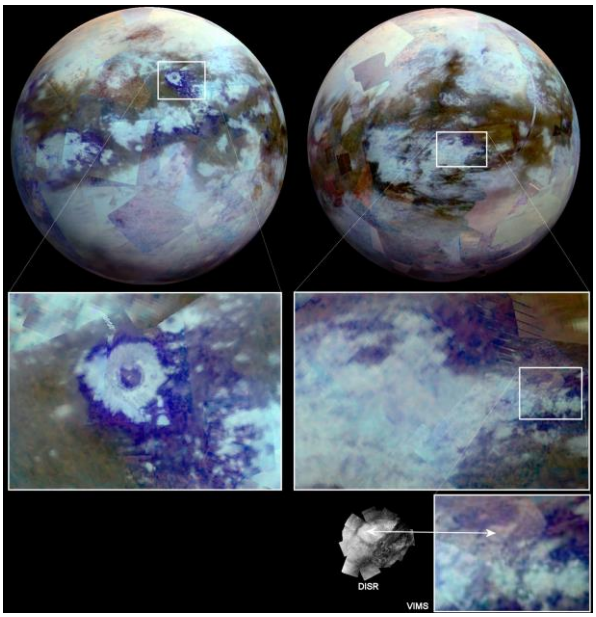

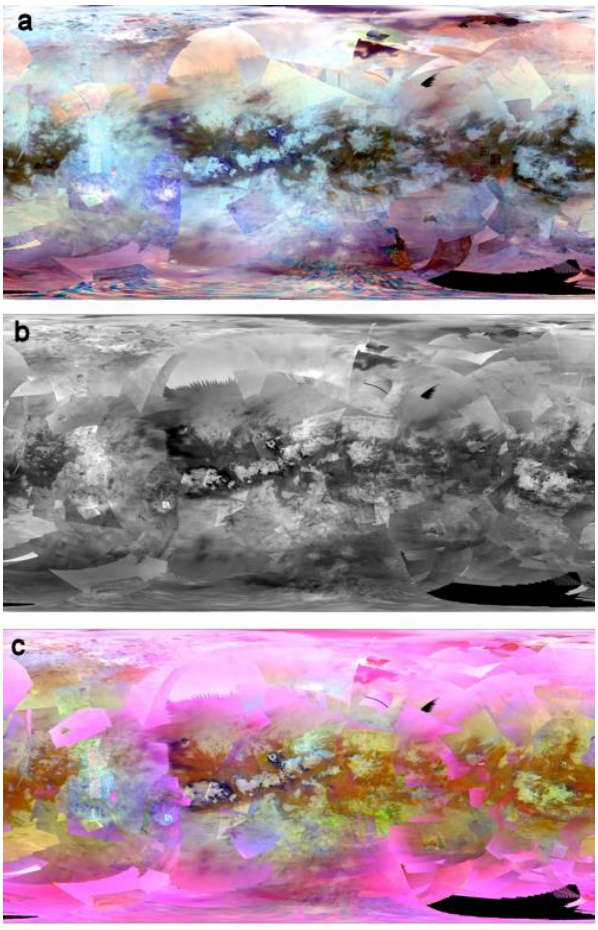

Fig.2 : (a) Global map with RGB controlled by the 5, 2 and 1.27 µm images corrected from scattering and photometry. *(b) 2.03/1.27µm ratio (c) RGB* controlled by the *1.59/1.27µm, 2..03/1.27µm, and B=1.27/1.08 µm. ratios.*

Fig. 3 (left) : orthographic views using the RGB map of Fig. 2a, with zooms on Sinlap crater (left) and the Huygens Landing site (right). The bright feature seen by DISR during its descent can be recognized in the VIMS mosaic.

References: [1] Brown R.H. et al., Space Sci. Rev., 115, 111-168, 2004. [2] Sotin C. et al., *Nature*, 435, 786-789, 2005. [3] Rodriguez S. et al., *PSS*, 54, 1510-1523, 2006. [4] Le Mouélic S. et al., *PSS*, 73, 178–190, 2012. [5] Rodriguez S. et al., Nature, 459, 2009. [6] Stefan K. et al., GRL 37, 2010. [7] Barnes J.W. et al., Planetary Sci., 2:1, 2013. [8] Cornet T. et al., EGU, abstract 7321, 2015. [9] Hirtzig M. et al., Icarus, 226, 470-483, 2013.